UC Irvine
UC Irvine Previously Published Works

Title

POISe: pulsed optoacoustic interferometric spectroscopy and imaging

Permalink

Journal

ISSN

Authors

Carp, Stefan A
Guerra, Arnold
Duque, Samuel Q
et al.

Publication Date

DOI

Copyright Information

Peer reviewed

POISe: Pulsed Optoacoustic Interferometric Spectroscopy and Imaging

Stefan A. Carp[a,c], Arnold Guerra III[c], Samuel Q. Duque Jr.[a] and Vasan Venugopalan[a,b,c]

[a]Department of Chemical Engineering and Materials Science, University of California, Irvine, Irvine, CA 92697;
[b]Department of Biomedical Engineering, University of California, Irvine, Irvine, CA 92697;
[c]Laser Microbeam and Medical Program, Beckman Laser Institute,
1002 Health Sciences Road East, Irvine, CA 92612

ABSTRACT

POISe is a spectroscopic imaging technique based on the measurement of surface motion resulting from thermoelastic stress waves produced by short pulse laser irradiation of optically heterogeneous turbid samples. Here we show the capability of POISe to form tomographic images of tissue phantoms using surface displacement measurements taken at several locations following irradiation of a sample with a Q-switched Nd:YAG laser λ=1064 nm. The principal component of POISe is a modified Mach-Zehnder interferometer that provides surface displacement measurements with a temporal resolution of 4 ns and a displacement sensitivity of 0.2 nm. By performing simple image reconstructions on data sets acquired from several tissue-like phantoms, we demonstrate the ability of POISe to provide better than 250 μm spatial resolution at depths of 6 to 8 mm in a strongly scattering medium (μ_s'=1/mm). This technique shows great promise for high-resolution non-invasive imaging of superficial ($<$ 1 cm) tissue structures.

Keywords: photoacoustic, interferometer, beam forming, image reconstruction, thermoelastic effect

1. INTRODUCTION

Optoacoustic tomography has emerged over the past 10 years as a medical technology that promises to image tissues with resolution on the order of hundreds of microns at tissue depths approaching several centimeters.[1–4] This technology is similar to ultrasound in that imaging is performed by detecting pressure waves on the surface of the body. However, rather than generating pressure waves using piezoelectric transducers as in ultrasound, optoacoustic imaging uses pressure waves produced by short pulse laser irradiation of tissue structures. Thus, while maintaining the high spatial resolution enabled by the relatively non-dispersive propagation of stress waves, optoacoustic imaging benefits from endogenous or exogenous optical contrast between tissue structures. By comparison, contrast in ultrasound images originates from acoustic impedance mismatches that are generally weak in soft tissues. Furthermore, since the propagation of the pump laser radiation is governed by multiple light scattering, optoacoustic methods can potentially image up to tissue depths comparable with those achieved by diffuse optical methods such as photon migration.[5]

This paper describes a novel optoacoustic technique for imaging and physiological characterization of heterogeneous tissues at depths approaching 1 cm with a spatial resolution $<$ 250 μm. Unlike current optoacoustic implementations based on the detection of stress transients, our method uses an optical interferometric system to measure the surface displacement of a tissue sample in response to short pulse laser irradiation. The time-resolved surface movement is related directly to the spatial distribution of absorbed energy density in the sample. An additional advantage is that our approach requires no physical contact with the sample and has the potential to provide increased sensitivity and lateral resolution relative to current time-resolved stress detection approaches. This technique could presumably detect any tissue structure that possesses sufficient absorption or scattering contrast relative to their surroundings at a suitably chosen wavelength. Possible applications include detection and imaging of tumors and vascular lesions.

Send correspondence to Vasan Venugopalan
E-mail: vvenugop@uci.edu, Telephone: 1 949 824 5802, Fax: 1 949 824 2541

1.1. Current Optoacoustic Approaches

The underlying principle of optoacoustic imaging is the generation of stress waves by short pulse irradiation of a target with a pulse duration smaller than the acoustic transit time across the smallest physical feature that one wishes to image accurately.[4] Typically the time-resolved stress distribution at the boundary of the medium is measured using a variety of methods and used for image reconstruction. The classical approach to measuring the spatial and temporal pressure distribution is to use piezoelectric transducers placed in contact with the tissue surface.[2, 6–11] While this approach has been successful, there are some disadvantages. First, these transducers must remain in acoustic contact with the sample making detection of the stress waves on the same side as the laser irradiation cumbersome. Another drawback is that both the sensitivity of piezoelectric transducers and the horizontal resolution limit of the reconstructed image are proportional to the detector diameter. As a result a tradeoff exists between high sensitivity and high spatial resolution when using piezoelectric transducers.[11, 12] Alternate signal acquisition methods have been implemented, including optical detection of laser-induced stress waves[3, 13–15] and interferometric surface displacement tracking.[16–19] The former, while still a contact method can provide rapid acquisition of the stress field with high spatial resolution and over a relatively large field of view. The latter, which forms the basis for POISe, is a fundamentally different technology that measures the time-resolved surface displacement resulting from the absorption of laser radiation.

1.2. Pulsed Optoacoustic Interferometric Spectroscopy (POISe) and Imaging

POISe represents a continuation of our efforts represented by the work of Yablon and co-workers[17] as well as Payne and co-workers.[18, 19] At the core of the system is an interferometer capable of providing an absolute measurement of the time-resolved surface displacement with nanosecond temporal resolution and subnanometer displacement sensitivity. Apart from non-contact operation, POISe offers several other advantages. First, no calibration is required since the displacement is measured relative to the wavelength of the Helium-Neon laser which is known to better that 1 part in 10^6. Second, the probe beam of the interferometer can easily be focused down to a dimension ($\sim 10\ \mu$m) more than an order of magnitude smaller than the smallest piezoelectric transducers currently available. Thus high lateral resolution should be achievable without any loss of sensitivity.

2. MATERIALS AND METHODS

2.1. Experimental Setup

Figure 1 shows a schematic of the current POISe system. A pulsed pump laser beam irradiates the sample, generating the thermal expansion that is measured by a modified Mach-Zehnder interferometer in conjunction with associated electronics and a computer control system. The interferometer employs a polarized He-Ne laser (λ=632.8 nm), whose output is split by an acousto-optic modulator (ATM-1101A1, IntraAction) driven at 110 MHz. This setup has been previously described.[18, 19] Part of the He-Ne beam travels undisturbed through the AOM, while the rest is deflected into several frequency shifted beams. One of the first order frequency shifted beams ($\Delta f = 110$ MHz) is picked off by a mirror and forms the reference arm of the interferometer. The unshifted beam enters the sample arm of the interferometer, eventually reflecting off the sample surface. The polarization optics redirect the returning sample beam to recombine it with the reference beam at the 50/50 beamsplitter. The beams emerging from the beamsplitter are directed to two Si PIN photodiodes (Hamamatsu). The signal is further amplified using a broadband low-noise amplifier (Mini-Circuits) and digitized by a 500 MHz bandwidth digital oscilloscope (Tektronix).

When the sample surface is at rest, the interferometer signal is a sinusoidal oscillation at the AOM modulation frequency. However, the frequency of the oscillation is affected by movement of the sample surface through the Doppler effect. The time-resolved surface displacement $\mathbf{u}(t)$ is directly proportional to the instantaneous phase difference between the AOM driving signal and the interferometer signal. This relationship is given by[17, 18]:

$$\mathbf{u}(t) = \frac{\lambda[\Phi_{INT}(t) - \Phi_{AOM}(t)]}{4\pi} \tag{1}$$

where Φ_{INT} and Φ_{AOM} are the instantaneous phases of the interference and AOM driving signals, respectively and λ=632.8 nm for the HeNe laser. To this end both the interference and the AOM driving signal are digitized
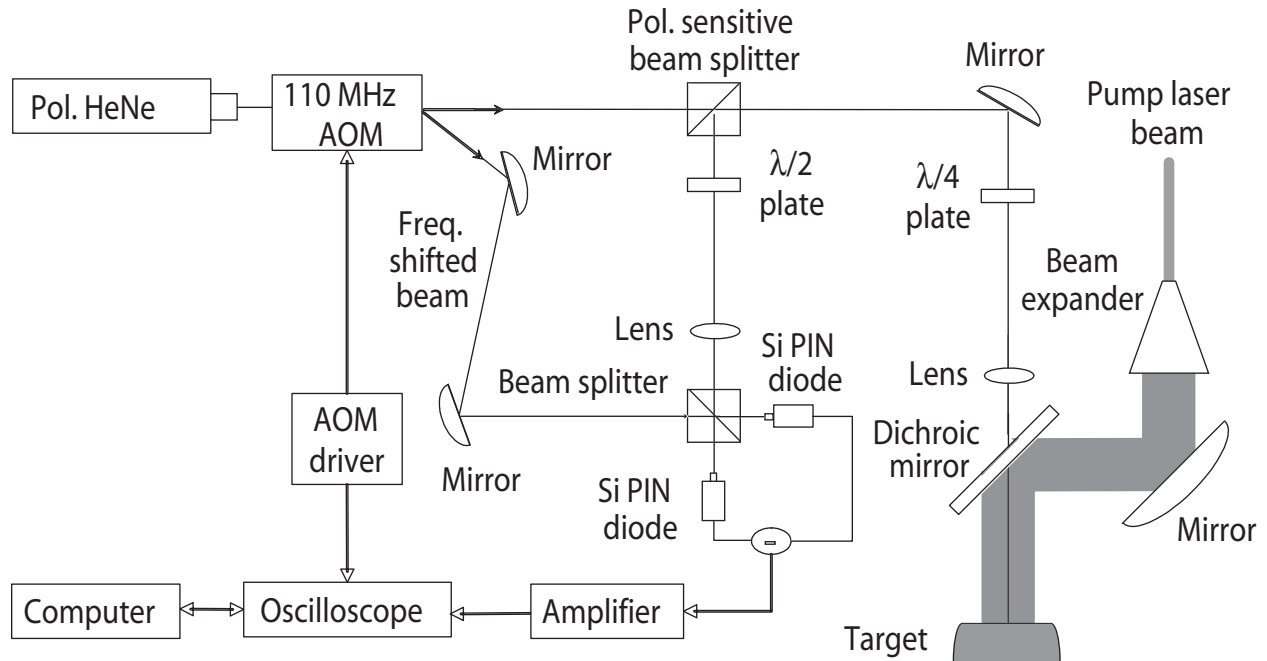
Figure 1. Schematic of the current POISe system. A Q-switched Nd:YAG laser operating at 1064 nm irradiates the sample, generating thermal expansion which is measured with an interferometric system employing a modified Mach Zehnder interferometer
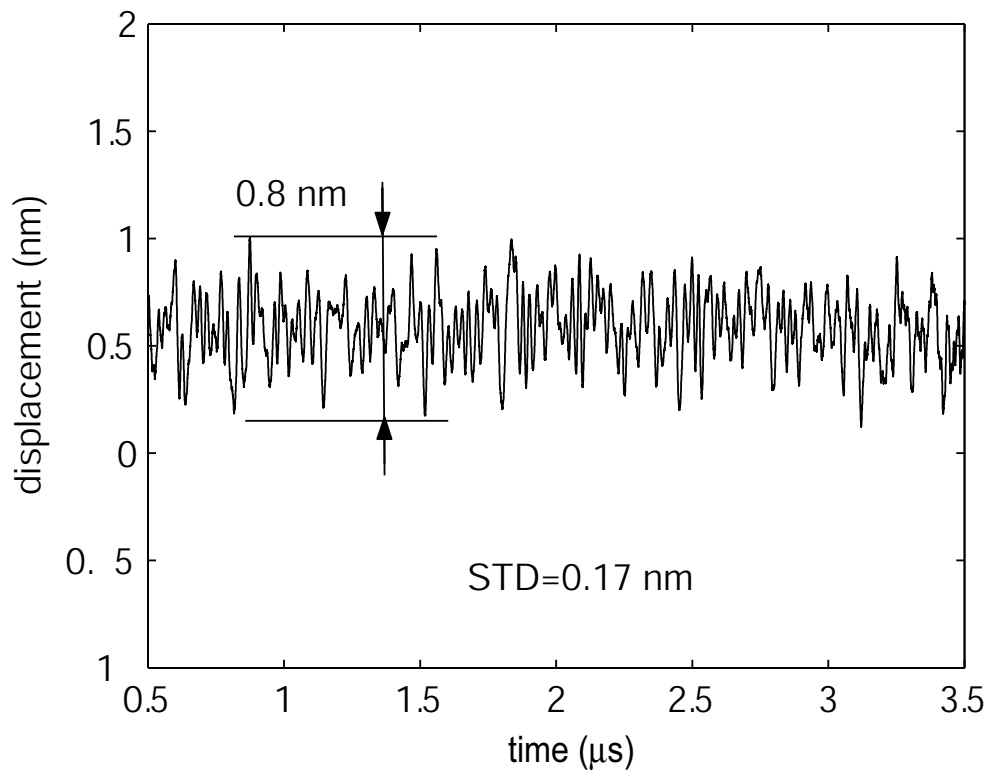
Figure 2. Sample interferometric trace from a stationary water surface. The displacement noise is within ± 0.4 nm, with a standard deviation of 0.17 nm
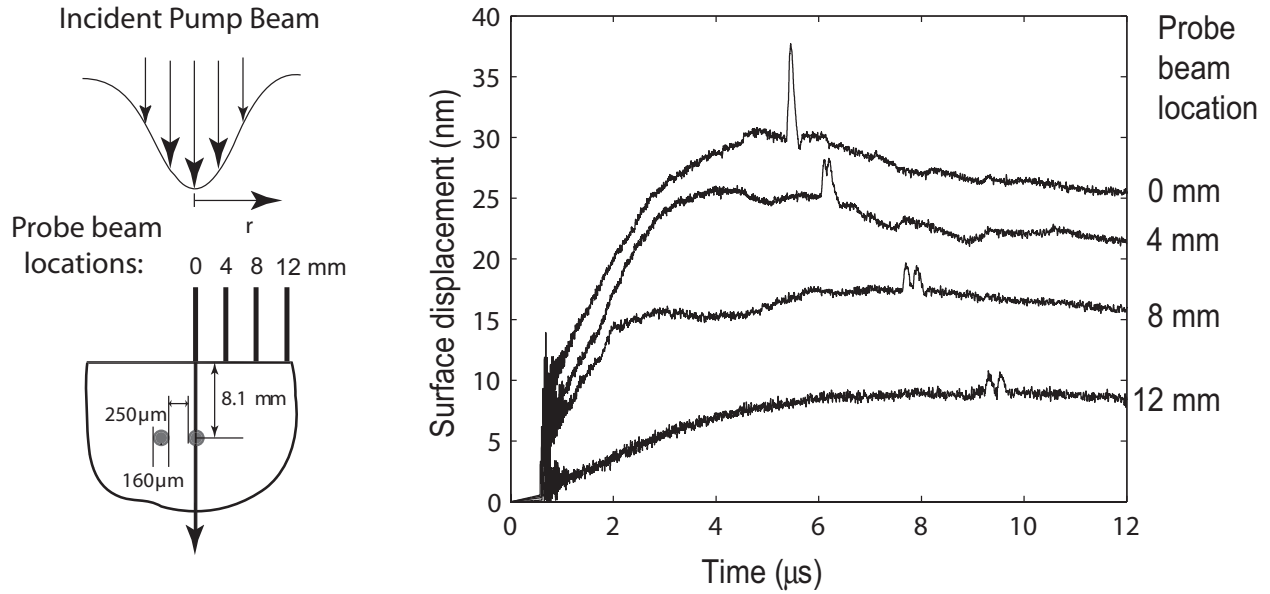
Figure 3. Displacement traces acquired at four different locations on the surface of a phantom containing two parallel polyimide tubes submerged 8.1 mm below the liquid surface.
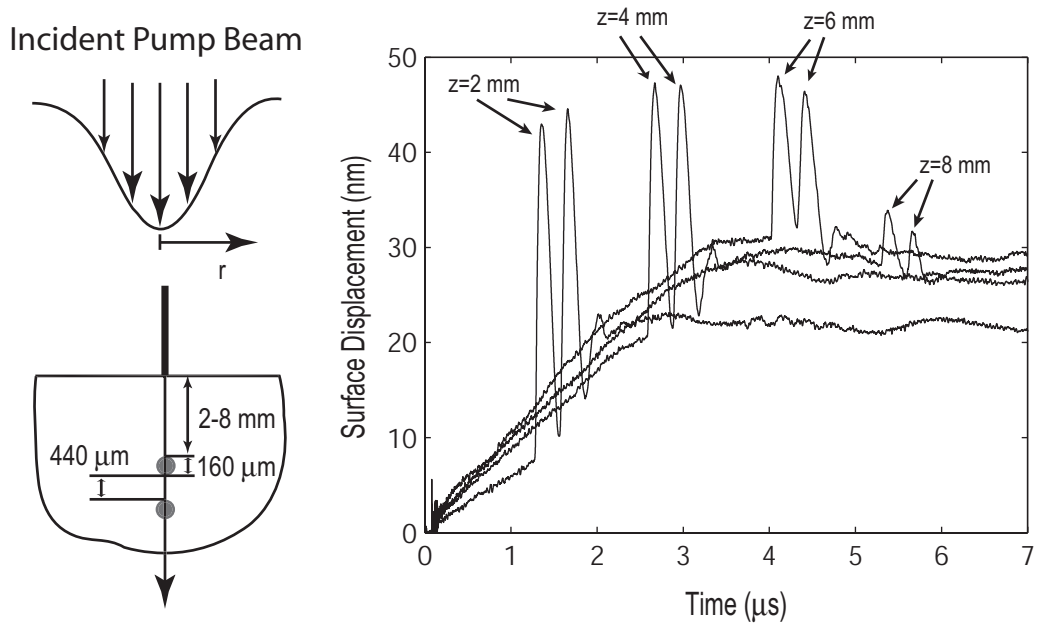
Figure 4. Displacement traces acquired on the surface of a phantom containing two stacked poylimide tubes. The upper tube was 2,4,6 or 8 mm below the phantom surface.

by the oscilloscope, and the instantaneous phase is determined using the Hilbert transform. Eq. (1) is then used to obtain the time-resolved surface displacement measurement. A single trace acquired without laser excitation on a water target is shown in Figure 2. Under these conditions the instrument routinely achieves a temporal-resolution of 4 ns and a displacement noise floor of $\pm$ 0.4 nm.

2.2. Phantom design

To examine the ability of POISe to detect and image heterogeneous structures, phantoms were constructed to simulate a pair of blood vessels immersed in a turbid tissue. The optical properties were targeted to mimic those of a typical tissue in the near-infrared. The scattering medium was a 2% Intralipid solution possessing a reduced scattering coefficient of μ'_s=1 mm^{-1}. Simulated vessels were fashioned using thin hollow polyimide tubes (Cole-Parmer) with an outer diameter of 160 μm and an internal diameter of 120 μm through which a dilute solution of India ink with μ_a=0.5 mm^{-1} was circulated to simulate the absorption of whole blood at λ=1064 nm. A Q-switched Nd:YAG laser (Quantel) operating at λ=1064 nm with a 5 ns pulse duration and 16.5 mm beam diameter (after expansion) was used as the pump laser beam with an incident radiant exposure of 100-200 mJ/cm^2. At this wavelength the polyimide tubes are essentially transparent, and their contribution to the displacement signal is negligible.

2.3. Image reconstruction principles

We employed a simple delay and sum beam-forming algorithm to reconstruct images from multiple surface displacement measurements acquired at distinct locations.[2] First we removed the displacement baseline due to homogeneous background absorption by fitting the initial rise in the displacement traces (see §3.1) to an exponential function $u(t) = A[1 - \exp(-Kt)]$ where A and K are fitting parameters. The tissue volume was then divided into small volume elements (voxels) and each of them was evaluated as a potential source from which a thermoelastic disturbance can emanate and be detected by measurements taken at different locations on the tissue surface. The delay and sum method determines the acoustic source intensity for each voxel by finding the time window within each detector trace that corresponds to the interior of the current voxel and performing a weighted sum of the averaged displacement signals in that window for all the detectors,

$$I(\boldsymbol{r}) = \frac{\sum_i w_i^d \left\langle S_i \left[\frac{(\boldsymbol{r}_i^d - \boldsymbol{r}) - l/2}{c_a} : \frac{(\boldsymbol{r}_i^d - \boldsymbol{r}) + l/2}{c_a} \right] \right\rangle}{\sum_i w_i^d} \tag{2}$$

where $\boldsymbol{r}$ is the location in the imaged volume, $I(\boldsymbol{r})$ is the acoustic source intensity corresponding to location $\boldsymbol{r}$, $\sum_i$ denotes a sum over all the detection points, w_i^d is a detector specific weighting factor, $S_i(t)$ is the time-resolved signal from the ith detector, $\boldsymbol{r}_i^d$ is the location of the ith detector, c_a is the speed of sound and l is the voxel size, : denotes the set of discrete displacements acquired within the time window of interest, and $<$ $>$ denotes averaging the signal over the time interval corresponding to the transit time accross the voxel in question. The set of weights w_i^d can be used to improve different characteristics of the formed image by compensating, for example, for the effects of geometrical attenuation or acoustic absorption as the signal travels from the focus point to the individual detectors.

3. RESULTS AND DISCUSSION

3.1. Characteristics of raw measurements

Figures 3 and 4 show two sets of surface displacement traces collected from phantoms with adjacent and stacked polyimide tubes. In Figure 3 traces are shown for several locations of the interferometer probe beam using a phantom containing two parallel polyimide tubes at a depth of 6.7 mm. The initial increase in the surface displacement is due to optical absorption by the aqueous intralipid solution. The two polyimide tubes produce two separate peaks at times corresponding to the acoustic transit time between each tube and the position of the probe beam. When the probe beam is positioned directly above the objects (r=0) the two peaks overlap and appear as one broadened peak. As the measurement position moves laterally away from the center of the vessels, the difference between the distances from the detection point to the two individual absorbers increases
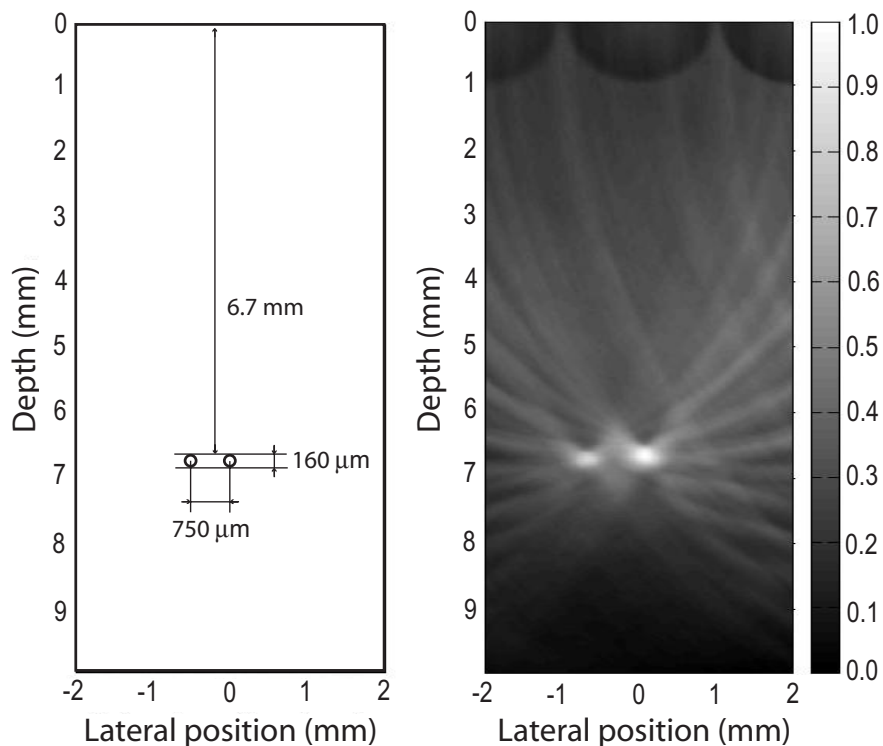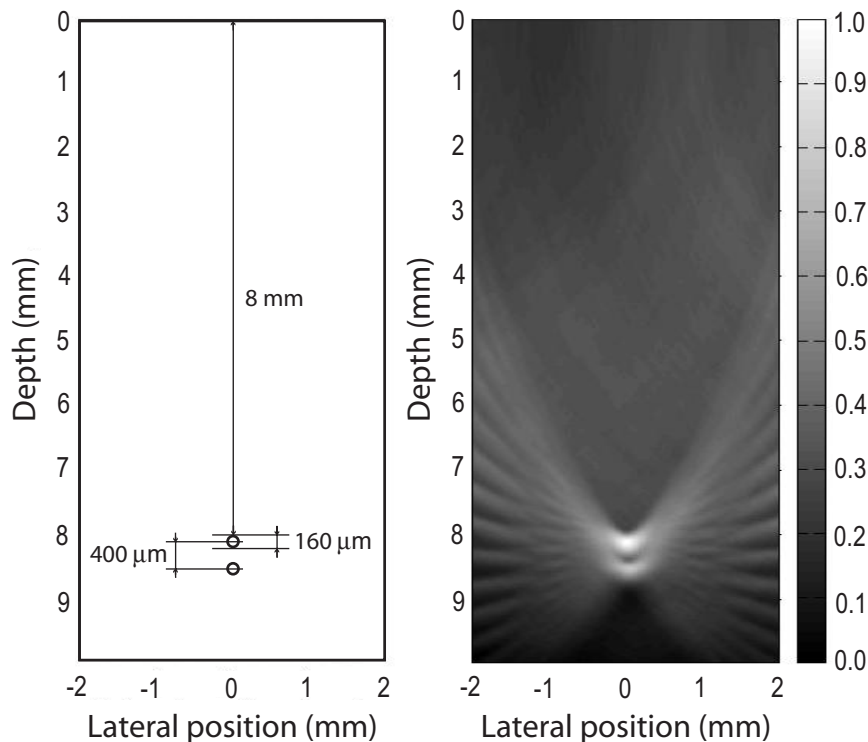
Figure 5. Image reconstruction performed on a phantom containing two parallel polyimide tubes submerged 6.7 mm below the phantom surface.

and the contributions to the displacement made by the individual tubes begin to separate in time. In this specific example complete separation is observed at $r = 12$ mm. Thus POISe is able to resolve two adjacent objects at depth if measurements are taken at sufficient lateral offsets. It is also important to note the sensitivity of the POISe measurement — the trace for $r = 12$ mm spans only 10 nm in displacement, and the peaks produced by the polyimide tubes measure only 2 nm and yet they are clearly distinguishable. Further noise reduction can be achieved by averaging a larger number of measurements as the traces shown here are the average of three individual acquisitions.

Figure 4 displays another notable achievement of POISe — its capability to distinguish absorbing objects in a stacked configuration. Traces are shown for measurements made with two stacked tubes at various depths between 2 and 8 mm. In every instance, the measurement is made directly above the objects and the separation of the two absorbers is clearly evident in the displacement traces. It is notable that coherent imaging methods such as Optical Coherence Tomography would not be able to make this distinction because absorption by the upper tube would prevent any coherent light from reaching the lower tube. By contrast, POISe detects the transient stresses generated by optical absorption regardless of whether the light reaches the target directly or through multiple scattering.

3.2. Simple image reconstructions

Figures 5 and 6 show some of our initial imaging efforts. Figure 5 displays an image reconstructed using the delay and sum method from measurements taken on a phantom containing two parallel polyimide tubes displaced by 600 μm wall-to-wall and submerged at a depth of 6.7 mm. Figure 6 is a similar image formed from measurements taken on a phantom containing two stacked polyimide tubes, displaced 240 μm wall-to-wall with the upper tube at a depth of 8 mm. All images are formed by processing 15 measurements taken every 2 mm between -14 and +14 mm along a line perpendicular to the tube axes.

Figure 6. Image reconstruction performed on a phantom containing two stacked polyimide tubes, with the upper tube 8 mm below the phantom surface.

The quality of the image reconstruction is excellent and good resolution is maintained even at a depth approaching 1 cm. Some artifacts in the form of "arcing" are seen. They are fundamental to the nature of the reconstruction algorithm, and can be reduced by increasing the number of measurements taken. Noting that objects about 240 μm apart can be clearly distinguished indicates that the resolution of POISe is better than 250 μm. These images show the potential of POISe to image tissue structures deeply and with high resolution.

ACKNOWLEDGMENTS

REFERENCES

1. R. Kruger, P. Liu, Y. Fang, and C. R. Appledorn, "Photoacoustic ultrasound (paus)–reconstruction tomography," *Med. Phys.* **22**(10), pp. 1605–1609, 1995.
2. C. G. A. Hoelen and F. F. M. de Mul, "Image reconstruction for photoacoustic scanning of tissue structures," *Appl. Optics* **39**(31), pp. 5872–5883, 2000.
3. K. P. Kostli, M. Frenz, H. P. Weber, G. Paltauf, and H. Schmidt-Kloiber, "Optoacoustic tomography: time-gated measurement of pressure distributions and image reconstruction," *Appl. Optics* **40**(22), pp. 3800–3809, 2001.
4. A. A. Karabutov, E. V. Savateeva, and A. A. Oraevsky, "Optoacoustic tomography: New modality of laser diagnostic systems," *Laser Phys.* **13**(5), pp. 711–723, 2003.
5. D. A. Boas, D. H. Brooks, E. L. Miller, C. A. DiMarzio, M. Kilmer, R. J. Gaudette, and Z. Quan, "Imaging the body with diffuse optical tomography," *IEEE Signal Proc. Mag.* **18**(6), pp. 57–75, 2001.

6. A. A. Karabutov, N. B. Podymova, and V. S. Letokhov, "Time-resolved laser optoacoustic tomography of inhomogeneous media," *Appl. Phys. B-Lasers O.* **63**(6), pp. 545–563, 1996.

7. A. A. Karabutov, E. V. Savateeva, N. B. Podymova, and A. A. Oraevsky, "Backward mode detection of laser-induced wide-band ultrasonic transients with optoacoustic transducer," *J. Appl. Phys.* **87**(4), pp. 2003–2014, 2000.

8. G. Paltauf and H. Schmidt-Kloiber, "Pulsed optoacoustic characterization of layered media," *J. Appl. Phys.* **88**(3), pp. 1624–1631, 2000.

9. A. A. Oraevsky, S. L. Jacques, and F. K. Tittel, "Measurement of tissue optical properties by time-resolved detection of laser-induced transient stress," *Appl. Optics* **36**(1), pp. 402–415, 1997.

10. A. A. Karabutov, I. M. Pelivanov, N. B. Podymova, and S. E. Skipetrov, "Determination of the optical characteristics of turbid media by the laser optoacoustic method," *Quantum Electron.* **29**(12), pp. 1054–1059, 1999.

11. C. G. A. Hoelen, F. F. M. de Mul, R. Pongers, and A. Dekker, "Three-dimensional photoacoustic imaging of blood vessels in tissue," *Opt. Lett.* **23**(8), pp. 648–650, 1998.

12. A. A. Oraevsky, R. O. Esenaliev, S. L. Jacques, S. Thomsen, and F. K. Tittel, "Lateral and z-axial resolution in laser optoacoustic imaging with ultrasonic transducers," in *Proceedings SPIE.*, **2389**, pp. 198–208, SPIE, 1995.

13. G. Paltauf, H. SchmidtKloiber, and H. Guss, "Light distribution measurements in absorbing materials by optical detection of laser-induced stress waves," *Appl. Phys. Lett.* **69**(11), pp. 1526–1528, 1996.

14. G. Paltauf, H. Schmidt-Kloiber, K. P. Kostli, and M. Frenz, "Optical method for two-dimensional ultrasonic detection," *Appl. Phys. Lett.* **75**(8), pp. 1048–1050, 1999.

15. J. J. Niederhauser, D. Frauchiger, H. P. Weber, and M. Frenz, "Real-time optoacoustic imaging using a schlieren transducer," *Appl. Phys. Lett.* **81**(4), pp. 571–573, 2002.

16. D. Albagli, M. Dark, L. T. Perelman, C. von Rosenberg, I. Itzkan, and M. S. Feld, "Photomechanical basis of laser ablation of biological tissue," *Opt. Lett.* **19**, pp. 1684–1686, 1994.

17. A. D. Yablon, N. S. Nishioka, B. B. Mikic, and V. Venugopalan, "Measurement of tissue absorption coefficients by use of interferometric photothermal spectroscopy," *Appl. Optics* **38**(7), pp. 1259–1272, 1999.

18. B. P. Payne, V. Venugopalan, B. B. Mikic, and N. S. Nishioka, "Optoacoustic determination of optical attenuation depth using interferometric detection," *J. Biomed. Opt.* **8**(2), pp. 264–272, 2003.

19. B. P. Payne, V. Venugopalan, B. B. Mikic, and N. S. Nishioka, "Optoacoustic tomography interferometric detection using time-resolved of surface displacement," *J. Biomed. Opt.* **8**(2), pp. 273–280, 2003.